

Seismic Behavior of Schwedler Domes

¹Asmaa Falih Dakheel, ²Dr. Ihab Sabri Saleh

1,2 Civil Engineering Department, College of Engineering, University of Basrah, Basrah, Iraq.

Corresponding Author: asmaa.alasadi2@gmail.com

Abstract

Dome structures have been used extensively for long-span systems in industrial, residential, and military infrastructures for their ability to cover large areas without intermediate supports, their lightweight, and their splendid aesthetic appearance. The seismic behavior of such structures not only is directly related to the safety of a building but also has a huge influence on the safety of people. Therefore, it is necessary to understand the seismic behavior for these structures under seismic loads. In this study, the seismic behavior of single-layer steel reticulated spherical Schwedler dome subjected to three-directional earthquake ground motion was investigated. Two types of Schwedler domes were chosen for the analysis and design, Schwedler monoclinical dome (A-dome) and Schwedler bidirectional dome (B-dome). The finite element models were established using SAP2000 software version 24, fifty-four dome models resting on the earth with 60m span and rigid joints and having different geometric properties, including varying rise-to-span ratios (10, 20, and 30%), number of meridional ribs, and number of latitudinal rings were studied. The models were designed only for gravity loads, and then the natural vibration properties were studied, after that the seismic load was applied. The seismic performance of Schwedler dome models is analyzed based on linear time history analysis (LTH); and the dynamic responses have been investigated. The results show that A and B dome models have identical vibration modes and dynamic responses, and the rise-to-span ratio has great influence on the dynamic characteristics, the rise-to-span ratio of 30% is the most suitable ratio for height of Schwedler domes with 60m span among the three ratios (10, 20, and 30%). In general, Schwedler domes can efficiently resist seismic loads.

Keywords: dynamic strength failure; failure mechanism; severe earthquake; reticulated domes, Schwedler dome

1. Introduction

The increasing demands of lighter, stronger and cheaper structures have prompted many architects, scientists, engineers to seek new technology and building concepts to achieve these goals [1]. The recent researches focus on structural systems that derive their performance from their curved shape, dictated by the flow of forces [2]. These structures can be extremely thin, elegant, cost-effective, earth-friendly, and have a smaller carbon footprint, that is because of their ability to cover large spans with a small amount of construction material and their effective structural characteristics [3-5]. There are many literatures which studied domes from different structural and geometrical aspects. Sabri and Abdulzahra [6] studied the response of space steel double layers frames with different positioning of point loads using Time History Analysis. Salih et al. [7] investigated the structural behavior of orthogonal square pyramid space grid under dynamic load, in which pyramid units with a square base are used. Jasim et al [8] studied the linear stresses and deformations of ribbed dome. Saleb and Muhsen [9] proposed several types of ribbed domes to improve their resisting for seismic loads. Yu et al. [10] performed a research on failure mechanism of single-layer steel reticulated domes with the reinforced concrete substructure subjected to sever earthquakes. Ma et al. [11] investigated the dynamic behavior and a seismic design method for single-layer reticulated domes with semi-rigid joints. Valibeig et al. [12] examined the structural details of discontinuous double-shell domes and revealed the factors affecting them. Kaveh et al. [13] developed an algorithm for optimum design of domes considering the topology, geometry, and size of member section using the cascade-enhanced colliding bodies optimization method. In large-scale space steel structures, a large number of design variables are involved. Yan et al. [14] presented a method to identify the most critical member in a single-layer latticed dome, which in the context of progressive collapse is defined as the member whose removal causes the most severe damage. Xu and Ye [15] modified the Member Discrete Element

Method (MDEM) and perfected it for three aspects: the algorithm itself, loading and computational efficiency, and to accurately and quantitatively simulate the progressive collapse for large-span spatial steel structures. Nayak et al. [16] studied domes with and without opening. Openings provided at bottom of the dome allow to provide more open area than that at crown which are used for light and ventilation. Tian et al. [17] conducted progressive collapse tests on a scaled single-layer latticed Kiewitt-6 (K6) dome subjected to non-uniform snow load. The failure mode, dynamic response, and collapse mechanism of the tested dome were examined. Zhang et al. [18] investigated the bidirectional and tridirectional isolation systems of large-scale single-layer lattice domes for improving the structural seismic performance and structural vibration control technology. Lee et al. [19] investigated the wind pressure characteristics of an elliptical plan retractable dome roof. Nair et al. [20] investigated the effects of higher modes of multistorey substructures on the seismic response of dome gridshell roofs using response spectrum analysis. Qi et al. [21] studied blast-resistant design considerations for dome structures. The authors investigated the effect of blast load variability on the design value and the structural dynamic response. Fan et al. [22] investigated the applicability of the seismic provisions of the current codes for the nonstructural components (roofing panels and purlins) of single-layer spherical reticulated domes. Zhang and Zhao [23] assessed the seismic resilience of incomplete single-layer reticulated domes and indicated the most unfavorable construction stage, a new curve of recovery functionality and methodology of seismic resilience during construction were established in this study.

Despite a numerous existing theories and structural analysis methods, the structural behavior of domes remains quite uncertain. Domes, mainly Schwedler, lack of adaptable and complete investigation and analysis methods effectively explain the capability of domes. In the present study, the seismic behavior of two types of Schwedler domes with different geometrical parameters has been investigated to explore their efficiency in resisting the earthquake ground motions.

2. Modelling Details

Single layer reticulated (domes composed of bars [24]) Schwedler domes with two patterns of configuration A = Monoclinal Schwedler dome (Figure 2.1) and B = Bidirectional Schwedler dome (Figure 2.2), with 60 m span, having different rise-to-span ratios ($h/s=10\%,20\%,30\%$), number of meridional ribs ($N_n = 8, 12, 24$) which are corresponding to plane angles of ($45^\circ, 30^\circ, 15^\circ$) respectively, number of circumferential rings ($N_r = 4, 8, 12$). Steel rectangular hollow sections with rigid connections have been used for all structural members, each node has six degrees of freedom, which can translate along the x, y, z directions and rotate around the x, y, z axes. Although the dome is curved in appearance, but all members are straight members.

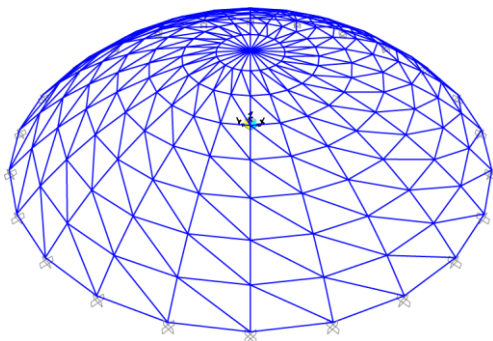


Figure 2.1 Monoclinal Schwedler dome

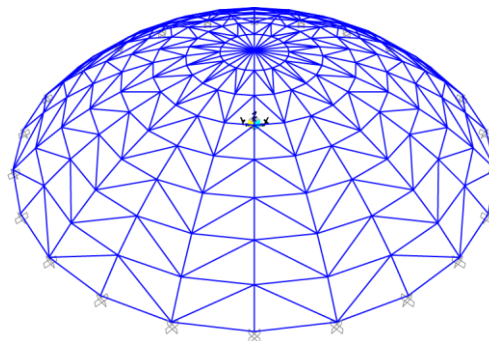
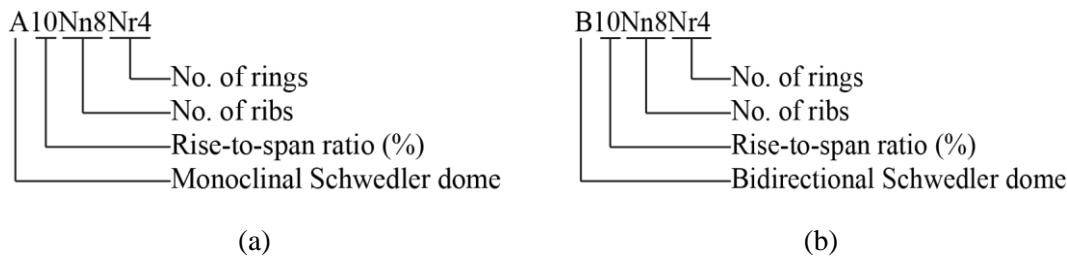


Figure 2.2 Bidirectional Schwedler dome

The simulation of the complex geometry of the space structure was done by using AutoCAD and SAP2000 Version 24 softwares. Two material properties were defined; one for structural members was steel ASTM A36 (Table 2.2) and the other for toughened glass panels (Table 2.3). Table 2.1 summarizes the different parameters of the models. Based on these parameters 54 dome models have been created, Figure 2.3 illustrates the label of analyzed models.

Table 2.1 Analysis parameters of Schwedler reticulated domes.

Parameter of Schwedler domes	Values of the parameter
Span (s)	60 m
Rise-to-span ratio (h/s)	10%, 20%, 30%
Rise	(6, 12, 18) m
Pattern of configuration (A and B)	A = Monoclinal Schwedler dome B = Bidirectional Schwedler dome
Plane angle	(45°, 30°, 15°)
No. of ribs	8, 12, 24
No. of rings	4, 8, 12
Earthquake	El Centro 1940

**Figure 2.3** Classification of single-layer reticulated Schwedler domes: (a) Monoclinal Schwedler dome (b) Bidirectional Schwedler dome.

2.1 Loading

2.1.1 Dead Loads

The dead load for the dome structure is primarily the own weight of structural members and the cladding. The structural members have been made of rectangular hollow sections. This type of cross section has been chosen because of its insensitivity to the lateral-torsion buckling and hence it is usually used in structures with glass covers [25]. The material used for structural members is steel ASTM A36, its mechanical properties are summarized in [Table 2.2](#).

Table 2.2 Steel ASTM A36 properties.

Yield tensile strength	250 MPa
Ultimate tensile strength	400 MPa
Young's modulus of elasticity	200 GPa
Material density	7850 kg/m ³
Poisson's Ratio	0.3

The glass panels were considered as thin concrete shell elements to simulate the limited lateral restraints to the hoops and ribs members [26]. [Table 2.3](#) illustrates the mechanical properties of toughened glass panels.

Table 2.3 Material properties for toughened glass panels [27].

Modulus of elasticity	70×10^3 N/mm ²
Compressive strength (F _{cu})	1000 N/mm ²
Tensile strength	120 N/mm ²
Material Density	25 kN/m ³
Linear coefficient of thermal expansion	$8 \times 10^{-6}/^{\circ}\text{C}$
Poisson's ratio	0.22
Thickness	10 mm

2.1.2 Live Loads

The minimum uniformly distributed live load for ordinary flat, pitched and curved roofs is given by ASCE 7-16 to be 0.96 kN/m² [28].

2.1.3 Seismic Loads

Seismic loads arise due to earthquakes. The reason of the seismic load on the structure is acceleration of the supports caused by acceleration of the ground [29]. The most critical seismic load effects can typically be computed using a three sets of ground motions, with two orthogonal components in each set that coincide with the global axes of the 3D model [28].

The three components of El Centro (Figure 2.4), 1940, earthquake ground motion are input into the structure in three directions as seismic load. The details of this earthquake are illustrated in Table 2.4.

Table 2.4 Details of the Imperial Valley earthquake ground motion at El Centro Array 9 station [30].

Earthquake Name	Year	Station Name	Magnitude, M_w	Peak ground acceleration, PGA (g)		
				(X-dir)	(Y-dir)	(Z-dir)
Imperial Valley-02	1940	El Centro Array 9	6.95	0.28	0.21	0.18

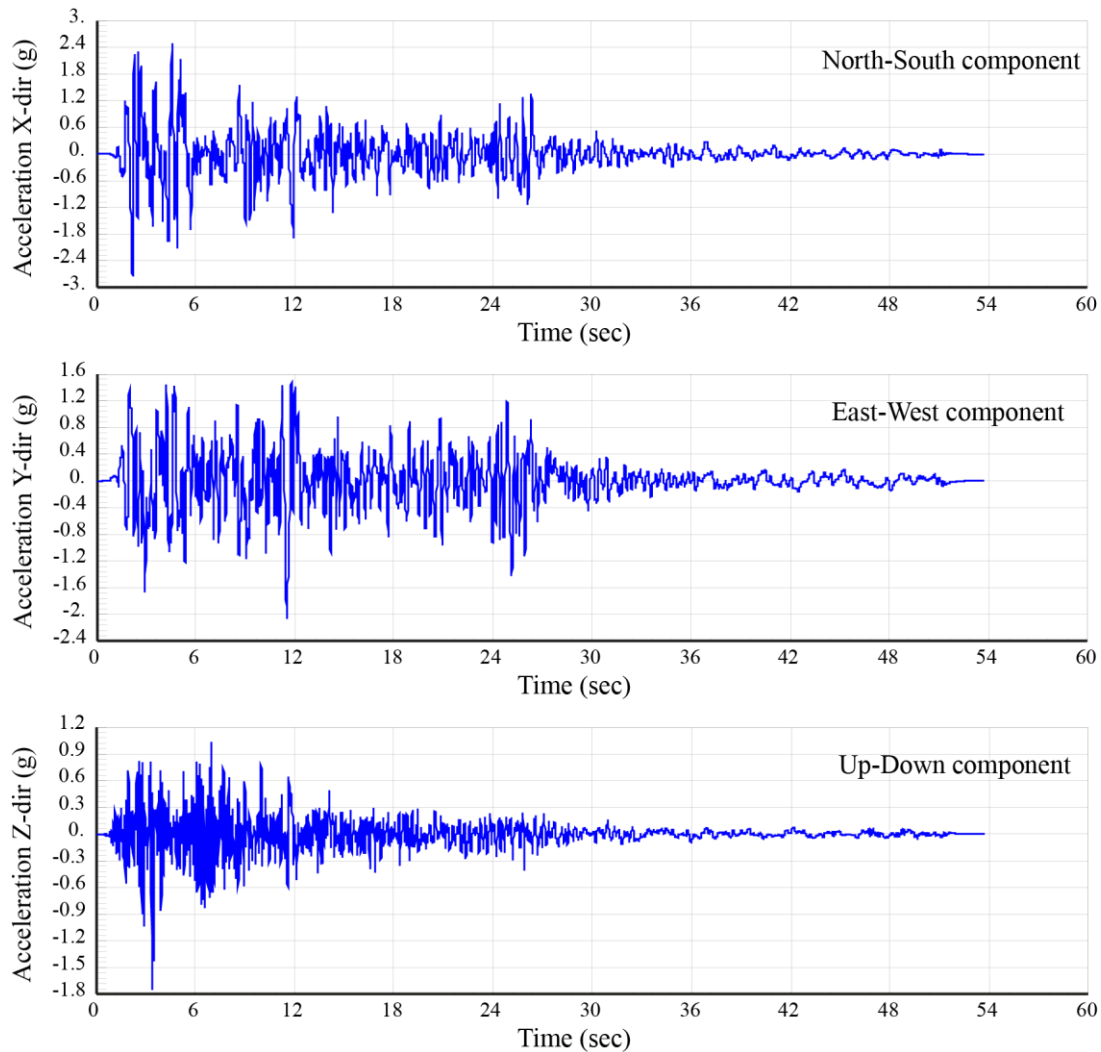


Figure 2.4 North–south and East–west components of horizontal ground accelerations and up–down component of vertical ground accelerations recorded at the El Centro Array 9 station, California, during the Imperial Valley earthquake of May 19, 1940.

3. Results and Discussion

3.1 Natural Frequency

As is well-known, free vibration frequency is one of the most important properties of the steel reticulated domes, and it influences the dynamic response of structures under earthquake actions. Therefore, the natural vibration frequencies are supposed to be studied first.

Figure 3.1 shows that the natural frequencies of Schwedler domes with 8 and 12 radial ribs and 4 latitudinal rings have frequencies larger than 90 cyc/sec, which have full response in x, y, and z direction with mass participation ratio of 90%, while the other models with natural frequencies less than 30 cyc/sec do not reach 90% of the mass participation ratio in any direction.

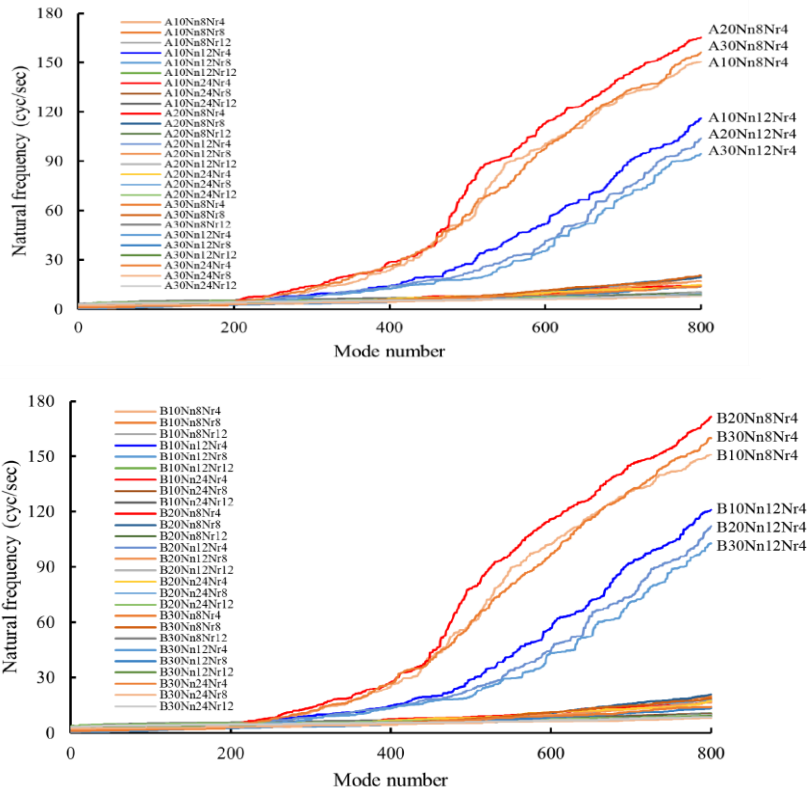


Figure 3.1 Natural frequencies of Schwedler domes with varying parameters.

3.2 Nodal Displacement

Structural displacement is one of the most important dynamic demands for the domes. Numerical results of maximum relative nodal displacement for 54 dome models, 27 models for each pattern of configuration of Schwedler domes, are presented in Table 3.1. These results are obtained by a dynamic linear time history analysis under three-directional seismic loading (El Centro, 1940).

Table 3.1 Maximum relative displacement in x,y, and z directions.

Model No.	Monoclinal Schwedler dome (A-dome)			Bidirectional Schwedler dome (B-dome)				
	Model	UX (mm)	UY (mm)	UZ (mm)	Model	UX (mm)	UY (mm)	UZ (mm)
1	A10Nn8Nr4	0.62	0.49	3.96	B10Nn8Nr4	0.79	0.63	3.79
2	A10Nn8Nr8	0.82	0.60	4.75	B10Nn8Nr8	0.83	0.60	4.98
3	A10Nn8Nr12	0.79	0.75	8.91	B10Nn8Nr12	0.80	0.70	8.69
4	A10Nn12Nr4	0.69	0.75	3.45	B10Nn12Nr4	0.90	0.92	3.84
5	A10Nn12Nr8	0.68	0.56	4.21	B10Nn12Nr8	0.80	0.60	4.28
6	A10Nn12Nr12	0.75	0.63	6.84	B10Nn12Nr12	0.82	0.70	7.55
7	A10Nn24Nr4	1.77	1.55	5.04	B10Nn24Nr4	1.33	1.17	4.06
8	A10Nn24Nr8	1.27	1.22	5.57	B10Nn24Nr8	1.26	1.08	4.22
9	A10Nn24Nr12	1.24	1.29	7.13	B10Nn24Nr12	1.40	1.28	6.10
10	A20Nn8Nr4	0.92	0.78	2.86	B20Nn8Nr4	1.22	0.80	2.28

11	A20Nn8Nr8	1.44	0.78	4.09	B20Nn8Nr8	1.63	0.98	3.08
12	A20Nn8Nr12	0.80	0.65	3.45	B20Nn8Nr12	0.67	0.52	3.30
13	A20Nn12Nr4	1.57	1.16	2.46	B20Nn12Nr4	1.51	1.32	3.15
14	A20Nn12Nr8	1.20	0.92	3.57	B20Nn12Nr8	1.23	1.00	3.53
15	A20Nn12Nr12	0.83	0.67	2.18	B20Nn12Nr12	0.95	0.78	2.85
16	A20Nn24Nr4	2.47	1.46	3.00	B20Nn24Nr4	2.03	1.34	2.52
17	A20Nn24Nr8	1.75	1.30	4.99	B20Nn24Nr8	2.19	1.42	3.45
18	A20Nn24Nr12	1.34	1.07	3.07	B20Nn24Nr12	1.66	1.58	2.65
19	A30Nn8Nr4	1.84	1.08	2.49	B30Nn8Nr4	1.57	1.04	2.33
20	A30Nn8Nr8	2.21	1.60	2.15	B30Nn8Nr8	2.06	1.48	2.65
21	A30Nn8Nr12	2.09	1.19	2.31	B30Nn8Nr12	2.08	1.25	2.69
22	A30Nn12Nr4	2.59	1.98	2.28	B30Nn12Nr4	2.68	2.00	3.71
23	A30Nn12Nr8	2.17	1.32	2.02	B30Nn12Nr8	1.88	1.28	2.70
24	A30Nn12Nr12	2.18	1.23	2.26	B30Nn12Nr12	2.24	1.14	1.96
25	A30Nn24Nr4	2.63	1.89	2.23	B30Nn24Nr4	2.89	2.05	1.88
26	A30Nn24Nr8	2.86	1.86	1.67	B30Nn24Nr8	3.36	1.96	2.02
27	A30Nn24Nr12	1.93	1.16	2.53	B30Nn24Nr12	1.67	1.08	1.92

3.3 Effect of Pattern on Dynamic Response

Comparison is made for the two patterns of configuration of Schwedler domes, A-pattern which refers to the Monoclinal Schwedler Dome and B-pattern which refers to the Bidirectional Schwedler Dome, Figure 4.20 shows that the two patterns are approximately behaving in the same manner in their dynamic response. That means that the pattern of configuration does not affect the dynamic properties.

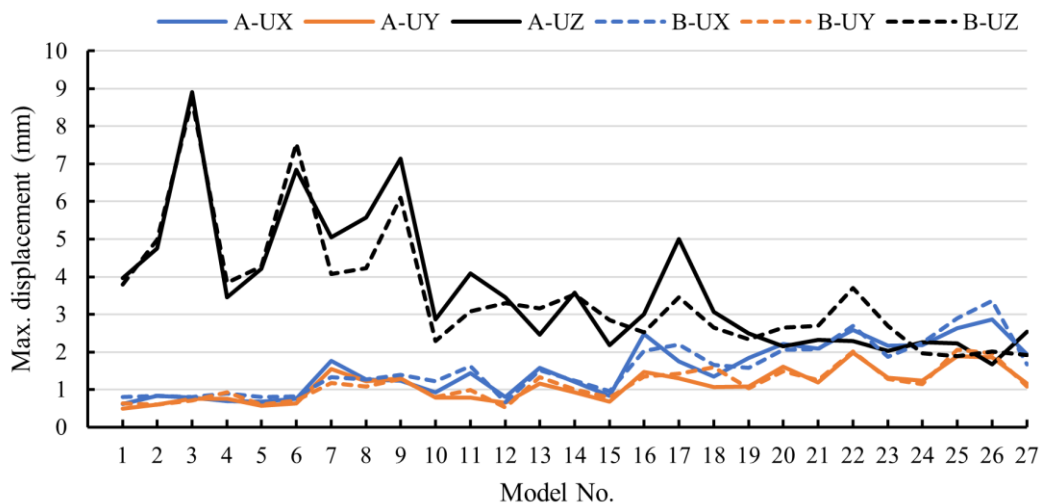


Figure 3.2 Effect of pattern of configuration of A and B models on dynamic displacement.

3.4 Effect of Rise-to-span Ratio on Dynamic Response

As a single-layer reticulated dome under seismic loading is sensitive to the change in shape, the rise-to-span ratio is a key factor having its influence on the shape of the structure. The rise-to-span ratio has also an important effect on the mechanical properties of the structure.

It can be clearly seen from Figure 4 for monoclinal Schwedler dome and Figure 5 for bidirectional Schwedler that displacement is significantly enhanced with the decreasing rise-to-span ratio, because the structure with a smaller rise-to-span ratio is flatter and so, the effect of horizontal seismic component is relatively reduced while the effect of vertical seismic component is increased. Consequently, the maximum nodal displacement of both reticulated Schwedler domes increases with the decreasing rise-to-span ratio, because the vertical vibration is the main vibration mode. The rise-to-span ratio of 30% is the most suitable ratio for height of Schwedler domes with 60m span among the three ratios (10%, 20%, and 30%) [Figure 3.3](#).

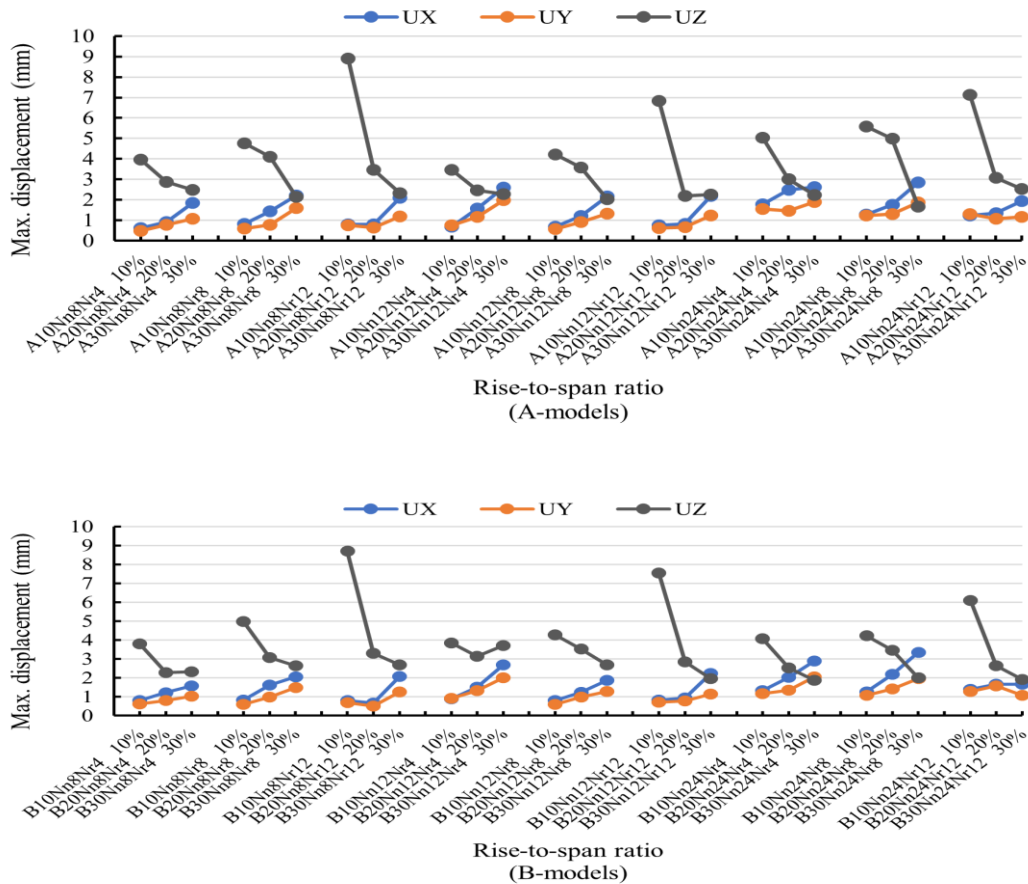


Figure 3.3 Maximum nodal displacement vs. rise-to-span ratio.

3.5 Effect of Number of Ribs on Dynamic Response

Three types of number of ribs ($N_n = 8, 12, 24$) corresponding to plane angles of (45, 30, 15), respectively, are considered in this study. The effect of N_n on max displacement of Schwedler domes is shown in Figures 4.60 and 4.61.

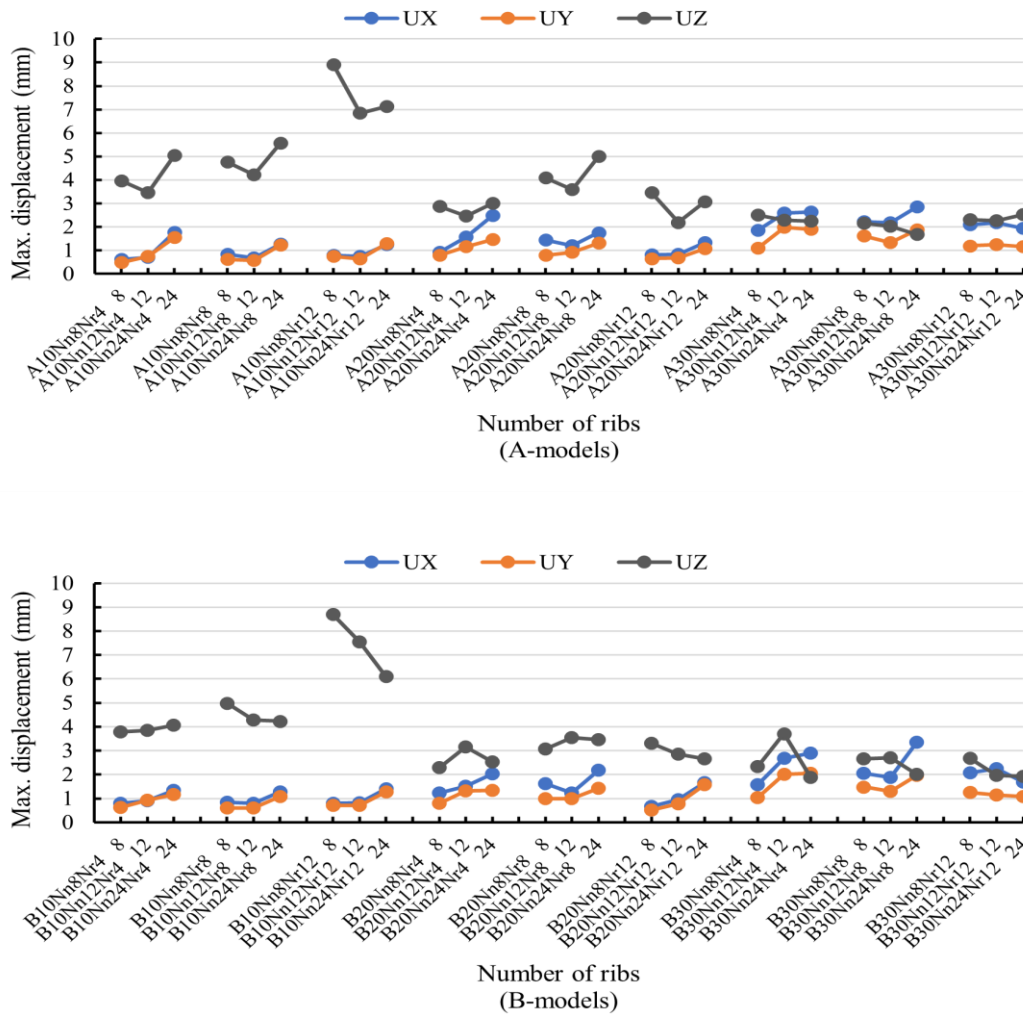
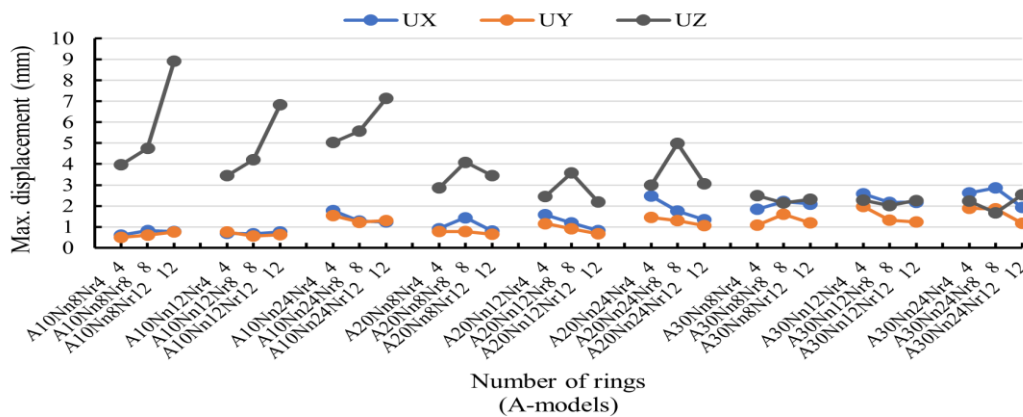


Figure 3.4 Maximum nodal displacement vs. number of ribs (Nn).

3.6 Effect of Number of Rings on Dynamic Response

The effect of increasing the number of rings on dynamic response is shown in Figures



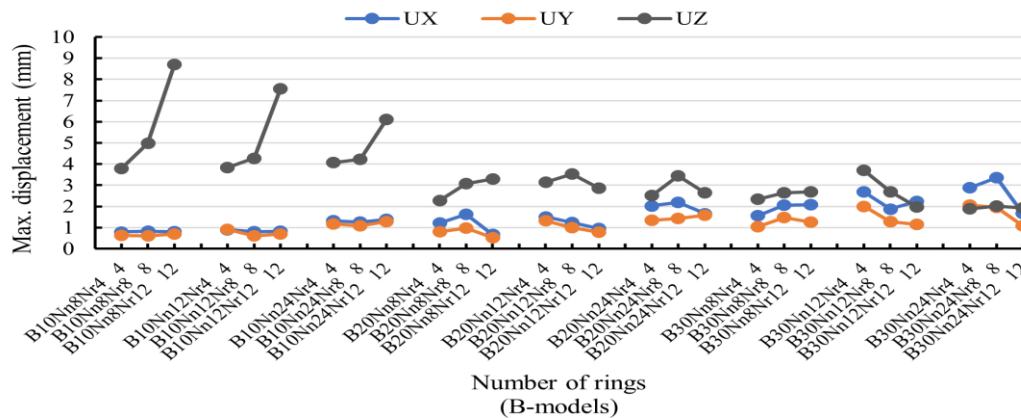


Figure 3.5 Maximum nodal displacement vs. number of rings (Nr).

4. Conclusions

Based on analyses results of single layer reticulated Schwedler dome models subjected to three-directional earthquake ground motion, the following conclusions and recommendations are drawn.

1. The pattern of configuration does not affect the dynamic properties.
2. The rise-to-span ratio of 30% is the most suitable ratio for height of Schwedler domes with 60m span among the three ratios (10%, 20%, and 30%).
3. Schwedler domes exhibit an outstanding performance in severe earthquakes. Light weight, appropriate geometry, redundancy, and large reserve strength are the key elements in such superior behavior.
4. The first mode is not necessarily dominant, and many higher order modes with close frequencies participate in the response, with many modes required to achieve an effective mass ratio of 90%. This makes it difficult to model the seismic response of lattice domes compared to ordinary multistory structures, which are often dominated by just a single mode.
5. As opposed to ordinary buildings, in Schwedler domes higher mode and vertical modes contribute in dynamic response effectively.
6. The models underwent a marked vertical displacement as they were subjected to three-directional excitation, whereas in ordinary buildings, there occurs no significant vertical displacement under three-directional excitation.

References

- [1] Z. Peng, "Geodesic Dome Structural Analysis and Design," *University of Southern Queensland*, 2016.
- [2] S. A. Behnejad, GAR Parke, and O. Samavati, *Inspiring the Next Generation - Proceedings of the International Conference on Spatial Structures (IASS2020/21-Surrey7)*. Spatial Structures Research Centre of the University of Surrey, 2022.
- [3] D. Pilarska and T. Maleska, "Numerical Analysis of Steel Geodesic Dome under Seismic Excitations," *Materials*, vol. 14, no. 16, p. 4493, 2021. [Online]. Available: <https://www.mdpi.com/1996-1944/14/16/4493>.
- [4] Y. Qiu, H. He, C. Xu, and B. San, "Aerodynamic optimization design of single-layer spherical domes using kriging surrogate model," *Advances in structural engineering*, vol. 24, no. 10, pp. 2105-2118, 2021, doi: 10.1177/13694332211992489.
- [5] S. Sote, "Structural Analysis of Dome Structure by STAAD Pro," *International Journal for Research in Applied Science and Engineering Technology*, vol. 9, no. 4, pp. 1515-1520, 2021/04/30 2021, doi: 10.22214/ijraset.2021.33990.

- [6] I. Sabri and Z. Abdulzahra, "Effect of Load Distribution on Dynamic Response of Double Layer Grids Space Steel Frames," 2015.
- [7] I. S. Salih, S. K. Faleh, and Z. A. Abdulrasool, "Effect of Type of Connection on Dynamic Response of Double layer Grid Space Frames," 2015.
- [8] N. A. Jasim, I. S. Saleh, and S. K. Faleh, "Structural Analysis of Ribbed Domes Using Finite Element Method," *International Journal of Civil Engineering Research*, vol. 8, no. 2, pp. 113-130, 2017.
- [9] I. Saleb and T. A. Muhsen, "Dynamic response of braced domes under earthquake load," *International Journal of Scientific and Engineering Research*, vol. 9, pp. 29-39, 2018.
- [10] Z. Yu, S. Li, D. Lu, C. Lu, and J. Liu, "Failure mechanism of single-layer steel reticular domes with reinforced concrete substructure subjected to severe earthquakes," *International Journal of Steel Structures*, vol. 16, no. 4, pp. 1083-1094, 2016/12/01 2016, doi: 10.1007/s13296-016-0025-8.
- [11] H. Ma, Z. Shan, and F. Fan, "Dynamic behaviour and seismic design method of a single-layer reticulated shell with semi-rigid joints," *Thin-Walled Structures*, vol. 119, pp. 544-557, 2017/10/01/ 2017, doi: <https://doi.org/10.1016/j.tws.2017.07.003>.
- [12] N. Valibeig, S. Rahravi Poodeh, and A. Rahimi Ariaei, "Structural and Geometric Analysis of Discontinuous Double-Shell Persian Domes in Isfahan and Nain Dome-Building Schools," *International Journal of Architectural Heritage*, vol. 11, no. 8, pp. 1101-1120, 2017/11/17 2017, doi: 10.1080/15583058.2017.1325540.
- [13] A. Kaveh, M. Rezaei, and M. Shiravand, "Optimal design of nonlinear large-scale suspendome using cascade optimization," *International Journal of Space Structures*, vol. 33, no. 1, pp. 3-18, 2018, doi: 10.1177/0266351117736649.
- [14] S. Yan, X. Zhao, K. J. R. Rasmussen, and H. Zhang, "Identification of critical members for progressive collapse analysis of single-layer latticed domes," *Engineering Structures*, vol. 188, pp. 111-120, 2019/06/01/ 2019, doi: <https://doi.org/10.1016/j.engstruct.2019.03.027>.
- [15] L. Xu and J. Ye, "DEM Algorithm for Progressive Collapse Simulation of Single-Layer Reticulated Domes under Multi-Support Excitation," *Journal of Earthquake Engineering*, vol. 23, no. 1, pp. 18-45, 2019/01/02 2019, doi: 10.1080/13632469.2017.1309606.
- [16] C. B. Nayak, M. A. Jain, and S. B. Walke, "Parametric Study of Dome With and Without Opening," *Journal of The Institution of Engineers (India): Series A*, vol. 101, no. 3, pp. 463-475, 2020/09/01 2020, doi: 10.1007/s40030-020-00447-3.
- [17] L.-m. Tian, J.-x. He, C.-b. Zhang, and R. Bai, "Progressive collapse resistance of single-layer latticed domes subjected to non-uniform snow loads," *Journal of Constructional Steel Research*, vol. 176, p. 106433, 2021/01/01/ 2021, doi: <https://doi.org/10.1016/j.jcsr.2020.106433>.
- [18] H. Zhang, X. Liu, H. Li, and N. An, "A comparative study on the effectiveness of bidirectional and tridirectional isolation systems used in large-scale single-layer lattice domes during earthquakes," *Soil Dynamics and Earthquake Engineering*, vol. 141, p. 106488, 2021/02/01/ 2021, doi: <https://doi.org/10.1016/j.soildyn.2020.106488>.
- [19] J. H. Lee, Y. C. Kim, D. J. Cheon, and S. W. Yoon, "Wind pressure characteristics of elliptical retractable dome roofs," *Journal of Asian Architecture and Building Engineering*, pp. 1-17, 2021, doi: 10.1080/13467581.2021.1941996.
- [20] D. Nair, K. Ichihashi, Y. Terazawa, B. Sitler, and T. Takeuchi, "Higher mode effects of multistorey substructures on the seismic response of double-layered steel gridshell domes," *Engineering structures*, vol. 243, p. 112677, 2021, doi: 10.1016/j.engstruct.2021.112677.
- [21] S.-b. Qi, G.-y. Huang, X.-d. Zhi, F. Fan, and R. G. J. Flay, "External blast load factors for dome structures based on reliability," *Defence Technology*, vol. 18, no. 2, pp. 170-182, 2022/02/01/ 2022, doi: <https://doi.org/10.1016/j.dt.2021.01.004>.

- [22] F. Fan, X. Zhi, and W. Li, "Analysis of the Acceleration Response Spectra of Single-Layer Spherical Reticulated Shell Structures," *Applied Sciences*, vol. 12, p. 2116, 02/17 2022, doi: <https://doi.org/10.3390/app12042116>.
- [23] T. L. Zhang and J. Y. Zhao, "Seismic Resilience Assessment of a Single-Layer Reticulated Dome During Construction," The Hong Kong Institute of Steel Construction, 2022/08/23 2022.
- [24] W. Gythiel, C. Mommeyer, T. Raymaekers, and M. Schevenels, "A Comparative Study of the Structural Performance of Different Types of Reticulated Dome Subjected to Distributed Loads," (in English), *Frontiers in Built Environment*, Original Research vol. 6, no. 56, 2020-May-22 2020, doi: 10.3389/fbuil.2020.00056.
- [25] B. Pokusiński and M. Kamiński, "Lattice domes reliability by the perturbation-based approaches vs. semi-analytical method," *Computers & Structures*, vol. 221, pp. 179-192, 2019/09/01/ 2019, doi: <https://doi.org/10.1016/j.compstruc.2019.05.012>.
- [26] M. M. Y. Kok Keong Choong and J. Y. R. Liew, *Recent Advances in Analysis, Design and Construction of Shell and Spatial Structures in the Asia-Pacific Region*. CRC Press, 2020.
- [27] F. Cobb, *Structural Engineer's Pocket Book*. CRC Press, 2020.
- [28] ASCE 7-16, *Minimum Design Loads and Associated Criteria for Buildings and Other Structures*. American Society of Civil Engineers, 2017.
- [29] I. A. Karnovsky and O. Lebed, *Advanced Methods of Structural Analysis*. Springer International Publishing, 2021.
- [30] D. R. Majhi and M. Shrikhande, "Residual life of earthquake damaged structures," *Soil Dynamics and Earthquake Engineering*, vol. 145, p. 106694, 2021/06/01/ 2021, doi: <https://doi.org/10.1016/j.soildyn.2021.106694>.